Switching Bonds in a DNA Gel: An All-DNA Vitrimer

Flavio Romano[1] and Francesco Sciortino[2]
[1]Physical and Theoretical Chemistry Laboratory, Department of Chemistry, University of Oxford, South Parks Road, Oxford OX1 3QZ, United Kingdom
[2]Sapienza–Università di Roma, Piazzale A. Moro 5, 00185 Roma, Italy
(Received 18 September 2014; published 19 February 2015)

We design an all-DNA system that behaves like vitrimers, innovative plastics with self-healing and stress-releasing properties. The DNA sequences are engineered to self-assemble first into tetra- and bifunctional units which, upon further cooling, bind to each other forming a fully bonded network gel. An innovative design of the binding regions of the DNA sequences, exploiting a double toehold-mediated strand displacement, generates a network gel which is able to reshuffle its bonds, retaining at all times full bonding. As in vitrimers, the rate of bond switching can be controlled via a thermally activated catalyst, which in the present design is very short DNA strands.

DOI: 10.1103/PhysRevLett.114.078104 PACS numbers: 87.14.gk, 81.07.Nb, 81.16.Dn, 87.15.A-

Nucleic acids have been recently employed as addressable building blocks to realize micro- and nanostructures with targeted properties. A variety of structures has been created via hierarchical self-assembly of nucleic acids [1,2], including stars [3], tiles [4], sheets [4], tubes [5], polyhedra [6–8], cages [9], as well as ordered (crystalline) [10] and disordered (gel) [11] bulk materials. DNA gels, the main subject of this Letter, have been realized by one-pot hierarchical self-assembly [11,12]. First, purposely designed single-stranded DNA sequences in solution (with a weight fraction of a few percent) join to form nanostars with the desired functionality. Then, these stars bind to each other, exploiting sticky-end recognition, originating a spanning network. The strength of the bonds can be varied by controlling the number of bases in the sticky end. From a technological point of view, DNA gels are biodegradable and nontoxic, and can reach elastic moduli of the order of a few pascal [13]. They can be made to encapsulate drugs, proteins, and even cells to provide controlled drug delivery [11]. DNA gels can also be used as an efficient medium for cell-free protein expression [11]. Additional applications of DNA gels to material science are discussed in Ref. [13].

Very recently, an innovative class of polymeric networks has been synthesized [14–16]. Differently from thermosets, which are made of permanently cross-linked polymers, these new plastics consist of a covalent network that can rearrange its topology via a bond-switching mechanism that preserves the total number of bonds [17]. When the bond switching is activated, the internal stress can be readily relaxed. A catalyst is used to control the rate of bond switching. The name vitrimer draws from their dynamical properties, which fall into the category of strong glass formers [18]; just like silica glasses, these materials can be heated and reworked to take any new shape without dissolving.

DNA is at the same time a genetic material and an inherently polymeric material made of a sequence of nucleotides. Along the lines of using DNA as a material [11,19], we describe in this Letter an innovative design of a vitrimer system entirely made of DNA sequences. In this DNA gel, bonds can switch without breaking, providing a mechanism for changing the network structure under an external driving force, retaining at all times the same number of bonds. To implement the bond switching mechanism, we use toehold-mediated displacement [20], one of the basic processes underlying dynamic DNA nanotechnology. Such mechanism has been recently exploited to control the lattice constant of nanoparticle crystals [21]. In toehold-mediated displacement, an incoming strand binds to a sequence of bases (the toehold) next to a double-stranded complex and then displaces one of the strands in the original complex through a branch migration process [22]. Finally, we show that control of the bond-switching rate can be achieved by adding in solution short DNA strands that act as temperature-driven inhibitors of the switching. This new DNA material thus acts as a cross-linked gel that can be reversibly turned into a flowing network with a small temperature (T) change around room T. In the following, we discuss: (i) the sequence design of the material; (ii) the design of the double-toehold mechanism which allows bond switching on the two different sides of the network node linker (see below); (iii) the evaluation of the switching rate of an isolated binding complex; and (iv) the design of the short DNA strands that inhibit switching at low temperature. We point out that the switching rate of an isolated binding complex is the only input required by a more coarse-grained model [23] in order to accurately reproduce the thermodynamic behavior of vitrimers, and is thus the crucial parameter to compute with a nucleotide-level detailed description of DNA.

The challenging part of the design is to devise a system that can at the same time reach full bonding but allow for a relatively fast bond switching. Similarly to vitrimers [14],

we start by creating a mixture of two types of DNA supraparticles with functionality four (tetramers) and two (bridges), as depicted in Fig. 1(a). Since DNA nanostars with different functionality have been previously realized [11,12], we only stress here that the double-stranded parts of the tetramer and of the bridge have to be long enough

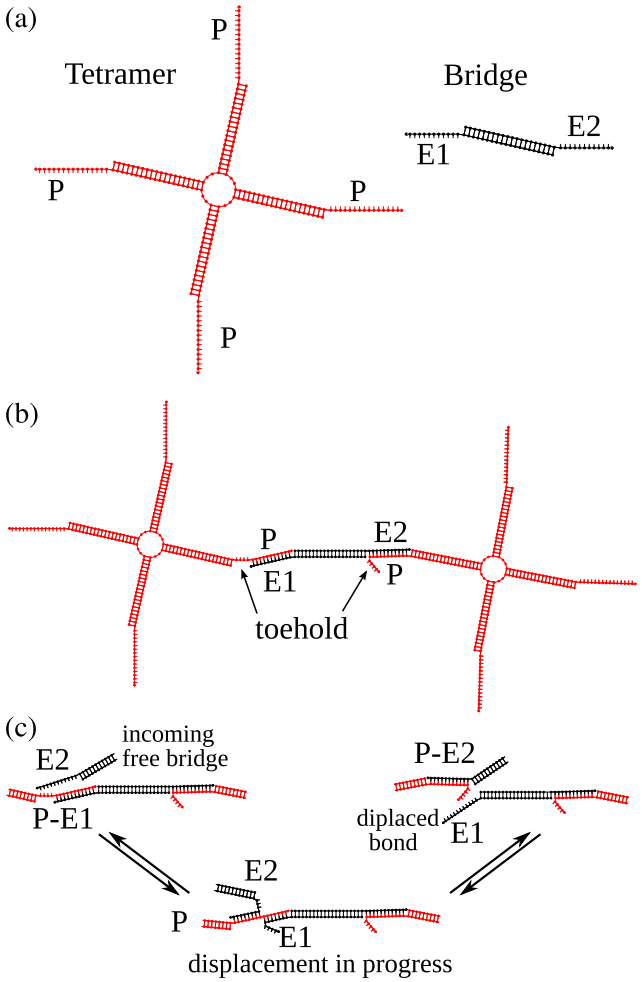

FIG. 1 (color online). (a) Tetramer and bridge particles. The tetramer (red) is composed of four DNA strands that bind to form a four-arm complex. Each arm terminates with an identical single-stranded sequence of 15 bases, labelled P. The bridge particle (black) is composed of two strands that bind to form a two-arm complex. The two arms terminate with two distinct sequences, $E1$ and $E2$ of 11 bases, complementary to different (partially overlapping) sections of P. (b) The tetramer and bridge arm sequences bind very strongly (11 base pairs) to form a network in which the tetramers correspond to the tetrafunctional nodes and the bridges provide the linking between different nodes. Note the two four-base toeholds next to the $E1$ and $E2$ sequences. Depending on whether $E1$ or $E2$ is bound to P, the toehold will be at the beginning or at the end of P. (c) Schematic representation of the switching mechanism. An incoming bridge particle (only a fraction is shown for clarity) attaches via the $E2$ sequence to the free toehold and progressively displaces the $E1$ sequence.

($\gtrsim$20 bases) so that their formation happens at a relatively high T, $T_{\mathrm{nanostar}} \gtrsim 80\,^{\circ}\mathrm{C}$.

For both types of particle, we design sequences such that each arm ends with an exposed single strand that allows binding between one of the arms of a tetramer and one of the arms of a bridge while leaving a short sequence of bases that will act as toehold. In the proposed design, the sequences exposed by the tetramer arms, named P, are all identical and composed of fifteen bases. The two sequences exposed by each of the bridge particles, $E1$ and $E2$, are distinct: they share an identical part of seven bases, preceded and followed, respectively, by two different terminal sequences of length four. Table I shows one optimal selection of bases for the $E1$, $E2$, and P sequences. These sequences are designed such that tetramer arms can bind only to bridge arms, while tetramer-tetramer and bridge-bridge bonds are forbidden. Moreover, P can bind via the same number of base pairs (11 bases) to either $E1$ or $E2$. In both cases, a four-base sequence on P is left unpaired to act as a toehold for the bond-switching mechanism. We encode two different toeholds per bond to avoid spurious toehold attachments: if the two toeholds were identical, the 5′ end of $E1$ would be able to attach to the free toehold of an existing P-$E1$ complex, but the displacement regions would be on opposite sides of the toeholds. This scenario is detrimental at low T, since a toehold is occupied with no possibility of displacement, and thus the switching rate needlessly suppressed.

By lowering T below T_{nanostar}, particles progressively aggregate, forming $E1$-P and $E2$-P bonds, to form a percolating network in which the nodes are the tetramers and the links are provided by the bridges [see Fig. 1(b)]. Below a certain T, T_{network}, all possible tetramer-bridge bonds allowed by their relative concentration will be formed. By selecting a nonstoichiometric concentration of bridge particles, e.g., [bridges] $>$ 2[tetramer], all tetramers will be bound to four bridge particles, whereas due to their excess concentration some of the bridge particles will have one or both of their ends free and thus are available for the switching process. The length of the $E1$-P and $E2$-P hybridized sections, 11 base pairs, guarantees that T_{network} is significantly separated from T_{nanostar}. At the same time, the 11-base length guarantees that (in the absence of the bond-switching mechanism), below T_{network}, the system is kinetically arrested in one network realization, as in a "chemical" (infinite bond lifetime) gel.

When a bridge particle with one free end comes close to another bridge particle which is bound, it can start binding to the toehold sequence and initiate the switching process, as shown graphically in Fig. 1(c). The optimal toehold length of four [20] is a compromise between a sequence that is long enough to be effective and at the same time short enough to guarantee that the transition (switching) state is transient. This bond-switching mechanism opens up

the possibility to rearrange the network without ever changing the total number of bonds.

We propose to modulate the switching rate r_{switch} by adding in the initial solution short strands, complementary to the toeholds, that will compete with the toehold-mediated displacement. At a low-enough T, T_{block}, binding of these short sequences becomes highly effective, completely blocking the switching process. We point out that T_{block} can be tuned independently of the other relevant Ts by varying the concentration of blocker strands, a parameter that does not affect the system otherwise.

The design of the sequences reported in Table I results from a series of considerations. $E1$, $E2$, and P should be able to form little unwanted secondary structure. This constraint is enforced to design a displacement mechanism as effective as possible. To design out unwanted secondary structure, we generate random sequences that have the desired secondary structure patterns, and then use NUPACK [24] to select those that have a total yield of unwanted secondary structure less than 5% at 40 °C. In our calculations, we assume a solution with a monovalent salt concentration of 0.5M, a value commonly used in experiments and also assumed in the oxDNA model [25,26] that we use. Finally, the two ends $E1$ and $E2$ of the linkers should have roughly the same affinity to the tetramer arms to provide a symmetric replacement process, even if we do not expect a small (1–2k_BT) asymmetry to affect the overall mechanism considerably. For this reason, we select the sequences that have a yield of $E1$-P bonds and $E2$-P bonds within 5% of one another.

To provide evidence that bond switching can take place in the T region where the network is fully bonded, we evaluate the free-energy profile of the bond-switching mechanism with simulations using the oxDNA model [25,26]. oxDNA is a quantitative coarse-grained model designed to reproduce thermodynamical, structural, and mechanical properties of single- and double-stranded DNA [20,27,28]. To estimate the bond switching rate, we simulate the switching process, i.e., the kinetics of a system with the P sequence bound to $E1$ evolving into a system with the P sequence bound to $E2$, and vice versa. More specifically, we simulate the fragments depicted in Fig. 1(c) (see Supplemental Material [29]), following the replacement process to completion. We evaluate the free-energy ($\beta\Delta f$) profile along a two-dimensional reaction coordinate based on the number of formed base pairs between P and $E1$ and between P and E2. To this aim, we apply umbrella sampling virtual move Monte Carlo simulations [30,31], where the perturbation added to the Hamiltonian is chosen to generate roughly equal sampling for all values of the reaction coordinate (see Supplemental Material [29]). The resulting two-dimensional free-energy profile is reported in Fig. 2(a) and in its projection along the minimum free-energy pathway in Fig. 2(b). The zero of $\beta\Delta f$ is chosen to coincide with the incoming bridge bonded to one of the toehold bases. We find that $\beta\Delta f$ first decreases, as the bridge binds more and more to the toehold, then it flattens off when the incoming bridge starts to compete with the original bridge connecting the two stars. At the end of the flat region, the incoming bridge has completely displaced the original, which remains still

TABLE I. Sequences used for the reactive ends of the tetramers (P) and bridges ($E1$ and $E2$). Both $E1$ and $E2$ can form 11 base pairs with P, leaving a toehold of 4 bases (TCAC or CCAA) at the end or at the beginning of P. The binding free energy is the same within $1k_BT$ at room T.

$E1$	5′-GGTTCGACACG-3′
P	3′-CCAAGCTGTGCTCAC-5′
$E2$	5′-CGACACGAGTG-3′

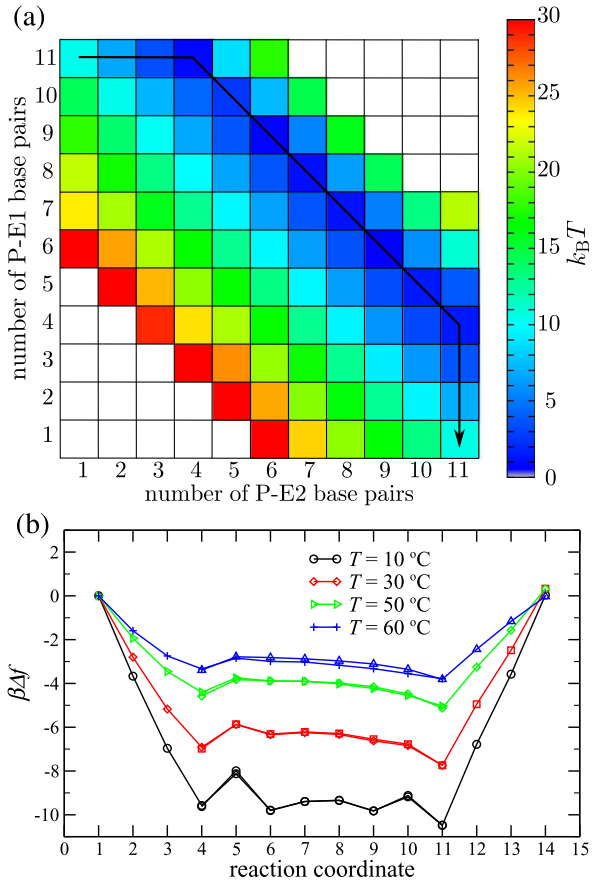

FIG. 2 (color online). (a) Free-energy profile at $T = 30$ °C. The two coordinates are the number of bonds formed by the incoming and original bridge to the tetramer reactive sequence. The pathway of lowest free energy for the displacement process (black continuous line) corresponds to a total of 15 interstrand base pairs. (b) Projection of the free-energy landscape along the pathway of lowest free energy. At low T, the detachment barrier is higher than $10k_BT$, while at intermediate T the barrier is smaller than $5k_BT$.

attached to its toehold. The flat region is characterized by small free-energy barriers at all T and the system oscillates between a fully bonded incoming bridge and a fully bonded original bridge. A rare event will eventually detach either the incoming bridge or the original one. We point out that the barrier to detaching, being related to the breaking of the four toehold base pairs, is T dependent and increases on cooling. The free-energy cost of forming the first contact (not shown in the figure; equivalent to the free-energy gain of the complete detaching) is dominated by the entropy loss of bringing the incoming bridges in close proximity to the toehold and it is thus linearly T dependent (i.e., constant $\beta\Delta f$ in Fig. 2).

The free-energy profile provides indication on the thermodynamic component of the switching rate. Its analysis suggests that the dominant contributions to the switching process are (i) the binding of the first nucleotide to the toehold (with a T-independent $\beta\Delta f$) and (ii) the activated process of completely detaching (with a T-dependent $\beta\Delta f$). These two processes, due to the significant free-energy barriers, are dominant with respect to the roughly T-independent time spent in the "flat" region of the energy profile. The free-energy profile shown indicate that the barriers for bond switching are not prohibitive, and thus it should be possible to observe the process via standard simulations. We indeed verified that this is the case. Simulating several hundred systems composed by a bonded P-$E1$ complex and a free $E2$ complex, we observed a few fully complete bond switchings within a few days. To accurately evaluate the displacement rate r_{switch}, we use forward flux sampling [28,32]. A detailed description of the method and of the associated assumptions is reported in the Supplemental Material [29]. Results for r_{switch} as a function of T are reported in Fig. 3. We find that r_{switch} is roughly constant, suggesting that the switching mechanism does not degrade on cooling and hence that the designed gel will be able to restructure itself below T_{network}. Although the absolute timings in the dynamics of coarse-grained models should not be overinterpreted, we report for convenience the absolute value for r_{switch} at $T = 20\,^{\circ}\text{C}$, which is $5 \times 10^4 \text{s}^{-1}$. We stress in passing that a full simulation of a DNA vitrimer is today unfeasible at the oxDNA level of detail. On the other hand, the bulk properties of a coarse-grained model vitrimer—in which r_{switch} was an input variable—composed of the same stoichiometric ratio of four and two functional particles as in the present case have been recently investigated [17]. Using the r_{switch} evaluated in this paper in combination with the model in Ref. [17] will provide a realistic description of the collective properties of a DNA vitrimer system.

Finally, we discuss the mechanism for controlling the switching rate, based on the action of additional short sequences (blocker strands) complementary to the two toeholds ($B1$ and $B2$, respectively). The bond-switching process requires both toeholds to be exposed, and thus if either of the toeholds is bound to a blocker strand the process is suppressed. Being only four bases long, the blocker strands attach to the toehold only at a low T, which can be tuned by acting on the concentration of the blocker strands to be well below T_{network}. The probability p_{bs}^{B1} (p_{bs}^{B2}) that $B1(B2)$ is bonded to a toehold, calculated with NUPACK [24], is shown in the inset of Fig. 3. The main panel of Fig. 3 shows the overall r_{switch} in the presence of blockers. Since the displacement can happen only if both blockers are not present, the overall r_{switch} is the product of the previously calculated r_{switch} multiplied by $(1 - p_{\text{bs}}^{B1})(1 - p_{\text{bs}}^{B2})$. In the presence of a blocker, r_{switch} is significantly reduced, effectively stopping the network rearrangements.

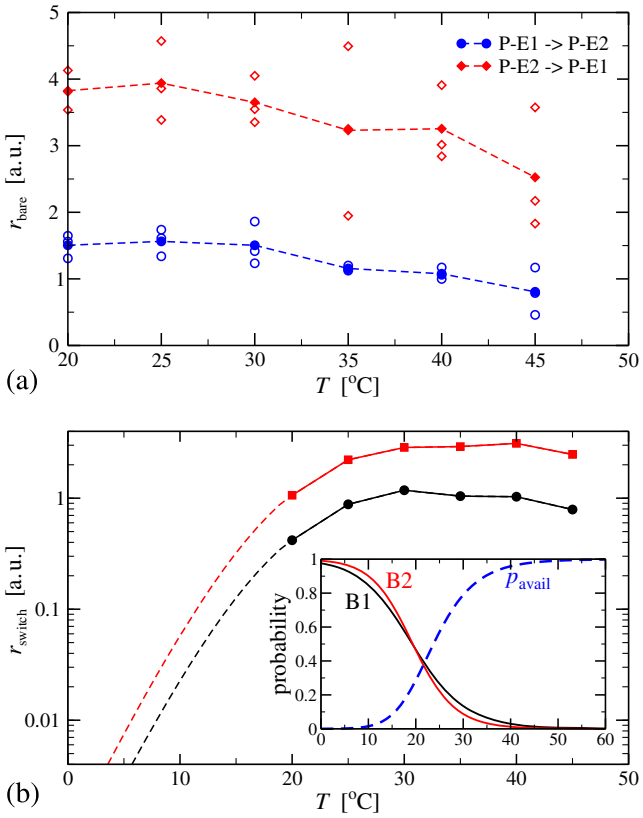

FIG. 3 (color online). (a) Displacement rate in the absence of blockers vs T for $E1$ replacing $E2$ and vice versa. Empty symbols represent the three individual rate measurements collected for each process, filled symbols represent their average. (b) Same, with blockers present. The dashed lines assume that the displacement rate in the absence of blockers is constant for $T < 20\,^{\circ}\text{C}$. The inset of (b) shows the probability of the two individual blocker strands being present, computed with NUPACK [24], and the probability $p_{\text{avail}} \equiv (1 - p_{\text{bs}}^{B1})(1 - p_{\text{bs}}^{B2})$ that none is present and thus the displacement can proceed. In line with Ref. [33], we assume a concentration of displacement complexes of 1 mM and an equal concentration of blocker strands.

In summary, encoding information into DNA sequences, we have designed a one-pot self-assembling all-DNA vitrimer, a gel made of DNA supramolecules which is able to restructure itself, self-healing any internal fracture via toehold-mediated strand displacement.

We acknowledge support from ERC-patchycolloids and the EPSRC for funding. We thank J. Doye, L. Leibler, T. Ouldridge, L. Rovigatti and F. Smallenburg for helpful discussions.

[1] Y. He, T. Ye, M. Su, C. Zhang, A. Ribbe, W. Jiang, and C. Mao, Nature (London) **452**, 198 (2008).
[2] S. H. Ko, M. Su, C. Zhang, A. E. Ribbe, W. Jiang, and C. Mao, Nat. Chem. **2**, 1050 (2010).
[3] N. R. Kallenbach, R.-I. Ma, and N. C. Seeman, Nature (London) **305**, 829 (1983).
[4] E. Winfree, F. Liu, L. A. Wenzler, and N. C. Seeman, Nature (London) **394**, 539 (1998).
[5] P. W. Rothemund, A. Ekani-Nkodo, N. Papadakis, A. Kumar, D. K. Fygenson, and E. Winfree, J. Am. Chem. Soc. **126**, 16344 (2004).
[6] R. P. Goodman, I. A. T. Sharp, C. F. Tardin, C. M. Erben, R. M. Berry, C. F. Schmidt, and A. J. Turberfield, Science **310**, 1661 (2005).
[7] C. M. Erben, R. P. Goodman, and A. J. Turberfield, J. Am. Chem. Soc. **129**, 6992 (2007).
[8] X. Li, C. Zhang, C. Hao, C. Tian, G. Wang, and C. Mao, ACS Nano **6**, 5138 (2012).
[9] C. Zhang, W. Wu, X. Li, C. Tian, H. Qian, G. Wang, W. Jiang, and C. Mao, Angew. Chem., Int. Ed. Engl. **51**, 7999 (2012).
[10] J. Zheng, J. J. Birktoft, Y. Chen, T. Wang, R. Sha, P. E. Constantinou, S. L. Ginell, C. Mao, and N. C. Seeman, Nature (London) **461**, 74 (2009).
[11] Y. H. Roh, R. C. Ruiz, S. Peng, J. B. Lee, and D. Luo, Chem. Soc. Rev. **40**, 5730 (2011).
[12] S. Biffi, R. Cerbino, F. Bomboi, E. M. Paraboschi, R. Asselta, F. Sciortino, and T. Bellini, Proc. Natl. Acad. Sci. U.S.A. **110**, 15633 (2013).
[13] J. B. Lee *et al.*, Nat. Nanotechnol. **7**, 816 (2012).
[14] D. Montarnal, M. Capelot, F. Tournilhac, and L. Leibler, Science **334**, 965 (2011).
[15] M. Capelot, M. M. Unterlass, F. Tournilhac, and L. Leibler, ACS Macro Lett. **1**, 789 (2012).
[16] Y.-X. Lu, F. Tournilhac, L. Leibler, and Z. Guan, J. Am. Chem. Soc. **134**, 8424 (2012).
[17] F. Smallenburg, L. Leibler, and F. Sciortino, Phys. Rev. Lett. **111**, 188002 (2013).
[18] C. A. Angell, Science **267**, 1924 (1995).
[19] N. C. Seeman, Nature (London) **421**, 427 (2003).
[20] N. Srinivas, T. E. Ouldridge, P. Šulc, J. M. Schaeffer, B. Yurke, A. A. Louis, J. P. K. Doye, and E. Winfree, Nucleic Acids Res. **41**, 10641 (2013).
[21] M. M. Maye, M. T. Kumara, D. Nykypanchuk, W. B. Sherman, and O. Gang, Nat. Nanotechnol. **5**, 116 (2010).
[22] D. Y. Zhang and G. Seelig, Nat. Chem. **3**, 103 (2011).
[23] F. Smallenburg and F. Sciortino, Nat. Phys. **9**, 554 (2013).
[24] J. N. Zadeh, C. D. Steenberg, J. S. Bois, B. R. Wolfe, M. B. Pierce, A. R. Khan, R. M. Dirks, and N. A. Pierce, J. Comput. Chem. **32**, 170 (2011).
[25] T. E. Ouldridge, A. A. Louis, and J. P. K. Doye, J. Chem. Phys. **134**, 085101 (2011).
[26] P. Šulc, F. Romano, T. E. Ouldridge, L. Rovigatti, J. P. K. Doye, and A. A. Louis, J. Chem. Phys. **137**, 135101 (2012).
[27] J. P. K. Doye *et al.*, Phys. Chem. Chem. Phys. **15**, 20395 (2013).
[28] T. E. Ouldridge, P. Šulc, F. Romano, J. P. K. Doye, and A. A. Louis, Nucleic Acids Res. **41**, 8886 (2013).
[29] See Supplemental Material at http://link.aps.org/supplemental/10.1103/PhysRevLett.114.078104 for a more detailed description of the model and of the computational techniques.
[30] G. Torrie and J. P. Valleau, J. Comput. Phys. **23**, 187 (1977).
[31] S. Whitelam, E. H. Feng, M. F. Hagan, and P. L. Geissler, Soft Matter **5**, 1251 (2009).
[32] R. J. Allen, C. Valeriani, and P. R. ten Wolde, J. Phys. Condens. Matter **21**, 463102 (2009).
[33] L. Rovigatti, F. Smallenburg, F. Romano, and F. Sciortino, ACS Nano **8**, 3567 (2014).